Innervation of Extraocular Pulley Smooth Muscle in Monkeys and Humans

Joseph L. Demer,† Vadims Poukens,‡ Joel M. Miller,§ and Paul Micevych‖*

Purpose. Soft pulleys stabilize paths and determine pulling directions of the extraocular muscles (EOMs). This study was conducted to characterize innervation of smooth muscles (SMs) supporting these pulleys.

Methods. Cadaveric human and monkey orbits were step and serially sectioned for histochemical and immunohistochemical staining. Before perfusion, the superior cervical ganglia of one monkey had been injected with the anterograde tracer *Phaseolus vulgaris* leukoagglutinin (PHA-L). Immunoperoxidase staining to human SM α-actin confirmed pulley SM. Monoclonal and polyclonal antibodies were used to demonstrate PHA-L, tyrosine hydroxylase, dopamine β-hydroxylase, phenylethanolamine-N-methyltransferase, neuronal nitric oxide synthase (NOS), and synaptophysin. The NADPH–diaphorase reaction was also used as a marker for NOS and the acetylcholinesterase (AChE) reaction for acetylcholine.

Results. Pulleys, consisting of collagen and elastin sleeves supported by connective tissue containing SM, were observed around rectus muscles of humans and monkeys. The human and monkey SM was richly innervated. Axons terminating in motor end plates within SM bundles were immunoreactive to PHA-L, tyrosine hydroxylase, and dopamine β-hydroxylase, but not phenylethanolamine-N-methyltransferase, indicating innervation of pulley SM from the superior cervical ganglion by projections using norepinephrine. Smaller axons and motor end plates were also demonstrated in SM, using NADPH–diaphorase and NOS immunoreactivity, indicating nitroxidergic innervation, and using AchE, indicating cholinergic parasympathetic innervation. The pterygopalatine and, to a lesser extent, the ciliary ganglia, but not the Edinger–Westphal nucleus, contained cells immunoreactive to NOS, suggesting that nitroxidergic innervation to pulley SM is mainly from the pterygopalatine ganglion.

Conclusions. The SM suspensions of human and monkey EOM pulleys are similar and receive rich innervation involving multiple neurotransmitters. These complex projections suggest excitatory and inhibitory control of EOM pulley SM, and support their dynamic role in ocular motility. Invest Ophthalmol Vis Sci. 1997;38:1774–1785.

Early radiographic studies in monkeys[1] and radiographic computed tomography in human subjects[2] first suggested that the bellies of the rectus extraocular muscles (EOMs) have paths that are stable in relation to the structure of the orbit, despite changes in gaze. This finding was unexpected because EOMs were thought to follow the shortest (great circle) path across the globe, limited somewhat by connective tissues.[3] This classic model predicted that "bridle forces" would, for example, give the horizontal rectus muscles an elevating action when the eye was in elevation. The stability of EOM paths was confirmed when the investigator used magnetic resonance imaging (MRI) with three-dimensional reconstruction to demonstrate a high degree of stability of rectus EOM belly paths throughout the physiologic range of human ocular rotations.[4] Only the anterior portions of the rectus tendons move in relation to the orbit—as they must to reach their insertions at the anterior part of the globe. Two possible mechanisms were hypothesized to explain the observed path stability of rectus EOMs: One involved connective tissue coupling to the

*From the *Jules Stein Eye Institute, Department of Ophthalmology and †Department of Neurology, University of California, Los Angeles; ‡Department of Pathology and Laboratory Medicine; §Smith–Kettlewell Eye Research Institute, San Francisco; ‖Department of Neurobiology, University of California, Los Angeles.*

Supported by National Eye Institute consortium grant EY-08313 (JLD, JMM), core grant EY-00331 to the Department of Ophthalmology at the University of California, Los Angeles, and core grant EY-06883 to Smith–Kettlewell Eye Research Institute.

Presented in part at the Association for Research in Vision and Ophthalmology, Sarasota, Florida, June 1995, and at the Society for Neuroscience, San Diego, California, November 1995.

Submitted for publication January 6, 1997; revised April 1, 1997; accepted April 2, 1997.

Proprietary interest category: N.

Reprint requests: Joseph L. Demer, Jules Stein Eye Institute, 100 Stein Plaza, University of California at Los Angeles, Los Angeles, CA 90095-7002.

Investigative Ophthalmology & Visual Science, August 1997, Vol. 38, No. 9

globe of an anterior extent of each muscle, and the other involved each muscle's passage through some sort of pulley coupled to the orbital wall.[5–8] In the latter case, orbital fat could increase the stability of the suspension by filling connective tissue interstices.[8,9] The first evidence for the pulley model was provided by MRI, demonstrating that EOM belly paths are minimally affected by large surgical transpositions of rectus tendons.[8] Because the surgical dissections divided all connective tissue attachments of the EOM tendons to the globe to a level at least 10 mm posterior to the insertions, it was concluded that EOM path stability was not caused by musculoglobal coupling. This excluded the first hypothesis. Improvements in MRI technique subsequently allowed pulley tissues to be directly visualized in humans, a finding that motivated a systematic reexamination of orbital anatomy in cadavers by gross and histologic techniques.[10]

Findings in recent anatomic studies indicate that each human pulley consists of a complete ring or sleeve of collagen encircling the EOM, located near the equator of the globe in Tenon's fascia.[10,11] Rectus tendons travel through their pulleys by sliding inside thin collagenous sheathes, which telescope within the pulley sleeves to permit passage of the entire tendon. Electron microscopic observations indicate that the collagen of pulley rings is extremely dense and is organized in an unusual configuration of perpendicular bands with directionally alternating fibrils; this structure is well-suited to high internal rigidity.[12] Located on the orbital side of each pulley ring is a dense mass of elastin and collagen. Pulleys are coupled to the orbital wall, adjacent EOMs, and equatorial Tenon's fascia by bands containing collagen and elastin, as well as smooth muscle (SM). The role of this SM has been unclear.

Smooth muscle has been described in classic orbital anatomic studies.[11–13] Müller[13] (cited by Page[14]) described SM in four areas of the human orbit: the inferior palpebral muscle, the superior palpebral muscle, the "orbital muscle" spanning the inferior orbital fissure, and the "peribulbar muscle" surrounding the anterior aspect of the globe. More recently, immunohistochemical staining for human SM α-actin has shown that SM cells are especially abundant in the suspensory bands of the pulleys[10] and may form part of what was described by Müller in the last century as the peribulbar muscle. Despite this similarity, the pulley SM cells are anatomically and structurally distinct from those of the more anterior palpebral SMs,[12] and those of the more posterior orbital muscle of Müller. In particular, the SMs around the medial rectus (MR) pulley are organized into bundles, unlike Müller's palpebral muscle.[12] Although the pulley is best developed for the MR muscle, all of the rectus EOMs have similar pulley structures in the vicinity of the equator of the globe.[10] The globe itself is supported trampoline-like by Tenon's fascia throughout its periphery by sturdy attachments to the periorbita, particularly at the orbital rim[10] and at the anterior and posterior lacrimal crests. In the human, the peripheral, equatorial portion of Tenon's fascia is a tough, fibromuscular structure composed of dense collagen, elastin, circumferentially arranged SM bundles, and some radially arranged SM bundles.[10]

Pulleys have important implications for EOM function.[10] Whereas the direction of pull (or resulting axis of rotation) of a rectus EOM was once thought to be determined by its anatomic origin in the annulus of Zinn, along with its point of tangency with the globe and the globe center, it now appears that the functional origin of an EOM is at its pulley. The length of a muscle's path, which (along with its resting length) determines the EOM's stretch and (along with innervation) its tension, is increased by deflection through its pulley. Although stiffened by elastin, the pulleys are compliant and would be subject to the action of their suspensory SMs and to changes in EOM tension. Although no functional role of the pulley SMs has yet been demonstrated, several candidate roles appear plausible. The SMs might simply regulate the stiffness of Tenon's fascia and the pulley suspensions to provide a constant load and geometry for the ocular motor system. Additionally, the SMs might move the pulleys to alter the pulling directions of EOMs, playing a dynamic role in slow eye movements.[10,12] For example, simulations of orbital biomechanics predict that small changes in pulley locations would have important effects on vergence.[15] The MR pulley appears to shift posteriorly during convergence and adduction (unpublished MRI data).

As a first step toward understanding the function of rectus pulley SMs, the current study was performed to compare the anatomy of pulleys in monkeys and in humans, and to investigate the types and sources of innervation of these SMs.

MATERIALS AND METHODS

Monkey Specimen Preparation

Two adult male monkeys, one fascicularis (*Macacca fascicularis*) and one rhesus (*Macacca mulatta*), were studied under a protocol approved by institutional animal welfare committees and adhering to the ARVO Statement for the Use of Animals in Ophthalmic and Vision Research. The fascicularis monkey had previously undergone implantation of a scleral magnetic-search coil for eye-movement recording studies and was killed by intravenous barbiturate overdose before intra-aortic perfusion with neutral-buffered saline at 0°C followed by 10% neutral-buffered formalin. The

head was then fixed for several days in 10% neutral-buffered formalin and the right orbit exenterated in an intracranial approach, as previously described for human specimens.[10] All visible bone fragments were removed with rongeurs under microscopic visualization. The orbit was then lightly decalcified for 12 hours in 0.003 M EDTA and 1.35 N HCl, embedded in paraffin, and serially sectioned at 10-μm thickness.

Ten days before death, the rhesus monkey was placed under barbiturate general anesthesia and the superior cervical ganglia bilaterally exposed.[16] Bipolar electrical stimulation was used to confirm identity of the superior cervical ganglion: Stimulation caused brisk pupillary mydriasis, whereas stimulation of the adjacent vagus nerve produced bradycardia as indicated by surface-lead electrocardiogram. Both superior cervical ganglia were then pressure-injected with 20 μl of the lectin *Phaseolus vulgaris* leukoagglutinin (PHA-L, Vector, Burlingame, CA) at a concentration of 2.5% in sodium phosphate-buffered saline (PBS) at pH 8. Surgical incisions were then sutured, and the animal recovered from anesthesia. Ten days later the monkey was killed by barbiturate overdose before perfusion with ice-cold phosphate-buffered saline followed by 4% neutral-buffered paraformaldehyde. The right orbit was exenterated en bloc, freed of bone fragments, and fixed in 10% neutral-buffered formalin for 4 days. The right orbit was lightly decalcified for 12 hours in 0.003 M EDTA and 1.35 N HCl, embedded in paraffin, serially sectioned at 10-μm thickness, and mounted on gelatin-coated slides.

The left orbit of the macaque was exenterated en bloc, and dissected to obtain tissue from pulley regions of each of the rectus EOMs and the ciliary ganglion. The right pterygopalatine ganglion, brain, adrenals, and both superior cervical ganglia were harvested. These specimens were fixed for 24 hours in 4% neutral-buffered paraformaldehyde, equilibrated in 30% neutral-buffered sucrose, serially sectioned at 10-μm thickness in a cryostat, and mounted on gelatin-coated slides.

Human Specimen Preparation

In conformity with relevant state and local laws, orbital specimens were obtained during authorized autopsy from five adult human cadavers within 8 to 12 hours of death. Gross dissection was performed in situ and after orbital exenteration. Specimens of EOMs and connective tissues were selectively dissected from some orbits and fixed in 4% neutral-buffered paraformaldehyde or 10% neutral-buffered formalin. Some fixed specimens were placed in 30% neutral-buffered sucrose before frozen sectioning at 10-μm thickness. Other specimens were embedded in paraffin and sectioned at 10-μm thickness. In an intracranial approach, both orbits of one cadaver were widely exenterated en bloc with periorbita intact.[8] Contents of the pterygopalatine fossa and the optic nerve posterior to the carotid siphon were included. The right orbit was similarly exenterated en bloc from two other cadavers. Bone was removed with rongeurs. One orbit from each cadaver was fixed in 10% neutral-buffered formalin for 4 days and lightly decalcified (12 to 20 hours) to soften the trochlea and any residual bone particles. Processing of control specimens verified that light decalcification does not interfere with subsequent staining procedures. The orbits were then dehydrated using graded solutions of alcohol and chloroform, embedded in paraffin, and serially sectioned at 10-μm thickness. The remaining orbit of the first cadaver was dissected before fixation to obtain specimens of pulley

FIGURE 1. (*top*) Whole 10-μm coronal orbital sections (oriented as a right eye seen from the anterior) stained with Masson's trichrome in three different primate species, illustrating similarity of connective tissue structures in pulleys and Tenon's fascia. Sections taken at a midglobal level best illustrate the medial rectus pulley ring (*open arrow*). Blue = collagen; red = striated muscle and lacrimal gland. (**A**) Human. IR = inferior rectus muscle; LG = orbital lobe of lacrimal gland; LPS = levator palpebrae superioris; LR = lateral rectus muscle; MR = medial rectus muscle; SO = superior oblique muscle; SR = superior rectus muscle. (**B**) Rhesus monkey. (**C**) Fascicularis monkey.

FIGURE 2. (*middle*) Immunoperoxidase stain for human smooth muscle α-actin in 10-μm coronal orbital sections near the medial rectus pulley. Hematoxylin counterstain. (**A**) Human orbit showing smooth muscle in equatorial Tenon's fascia (*inset*), and in focal bands extending from the pulley to the orbital wall and to the adjacent pulleys. (**B**) Rhesus orbit showing smooth muscle in equatorial Tenon's fascia (inset). Note cross-reactivity of monkey striated fibers (*open arrow*) to human smooth muscle antibody.

FIGURE 3. (*bottom*) Smooth muscles with blue nuclei are richly innervated by tyrosine-hydroxylase-positive axons (brown peroxidase reaction product; *arrows*) in the superior rectus pulley region of a human (**A**) and of a rhesus monkey (**B**), indicating synthesis of catecholamines. Hematoxylin counterstain, oil immersion.

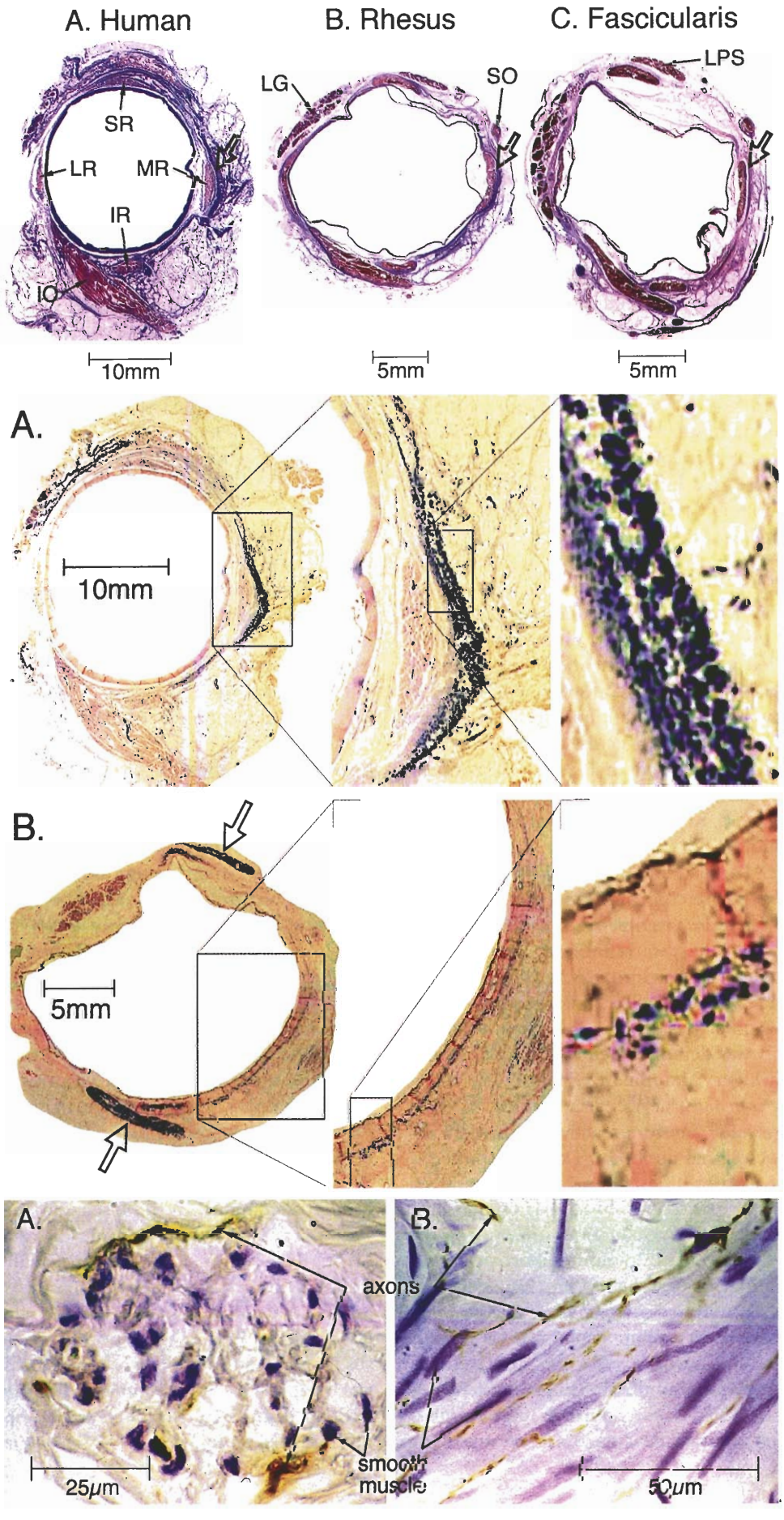
A. Human
B. Rhesus
C. Fascicularis
SR
LR
MR
IR
IO
LG
SO
LPS
10mm
5mm
5mm
A.
10mm
B.
5mm
A.
B.
axons
smooth muscle
25μm
50μm

tissues from around each of the rectus EOMs and the ciliary ganglion. Each of these selective specimens was then fixed for 24 hours in 4% neutral-buffered paraformaldehyde, equilibrated in 30% neutral-buffered sucrose, frozen in liquid nitrogen, and sectioned at 10-μm thickness in a cryostat.

Histochemistry

Step and serially sectioned 10-μm specimens were mounted on gelatin-coated glass slides. Masson's trichrome stain was used to show muscle and collagen, and van Gieson's stain to show elastin.[17] To demonstrate the NADPH–diaphorase reaction, mounted frozen sections were incubated in 0.1 M phosphate buffer, pH 7.4, containing 0.3% Triton X-100, 0.1 mg/ml nitroblue tetrazolium, and 1 mg/ml β-NADPH at room temperature for 30 to 60 minutes.[18] Some sections were lightly counterstained with nuclear fast red. To demonstrate acetylcholinesterase (AChE) activity, frozen sections were mounted on glass slides and processed as described.[19]

Immunohistochemistry

Smooth muscle was confirmed using monoclonal mouse antibody to human SM α-actin (Dako, Copenhagen, Denmark) applied at 4°C overnight at dilutions of 1:100 to 1:500. Nonspecific peroxidase was blocked using 3% H_2O_2 for 5 minutes. Antigen–antibody reactions were visualized using the ABC kit (Vector, Burlingame, CA) with diaminobenzidine (Sigma, St. Louis, MO) as the chromogen.[20] In some sections, blue chromogen Vector Alkaline Phosphatase Kit 3 (Vector) was also used to demonstrate human SM α-actin. Most sections contained vascular SM and striated EOMs, providing intrinsic positive and negative controls, respectively.

Tyrosine hydroxylase was demonstrated by immunoreactivity to a monoclonal mouse antibody (Incstar, Stillwater, MN), applied overnight at 4°C at a dilution of 1:300. Adrenal medulla and the intrinsic nerves of muscular arteries served as positive controls. Synaptophysin immunoreactivity was demonstrated with a monoclonal antibody (Bohringer–Mannheim, Mannheim, Germany), applied overnight at 4°C at a dilution of 1:10. Myelin basic protein immunoreactivity was demonstrated with a polyclonal antibody (Dako, Carpinteria, CA) for 1 hour at room temperature at a dilution of 1:50. Myelinated peripheral nerve was used as a positive control.

Dopamine-β-hydroxylase immunoreactivity was demonstrated with a polyclonal antibody (Eugene Tech, Ridgeford Park, NJ) applied at 4°C, either at a dilution of 1:250 overnight, or at a dilution of 1:500 for 2 days. Phenylethanolamine-N-methyltransferase was demonstrated using a polyclonal antibody (Eugene Tech) applied overnight at 4°C at a dilution of 1:1000. Adrenal medulla was used as a positive control for dopamine β-hydroxylase and phenylethanolamine-N-methyltransferase.

Phaseolus vulgaris leukoagglutinin (PHA-L) is a plant lectin that undergoes anterograde transport in neurons.[21] To trace projections from monkey superior cervical ganglia that had been injected with PHA-L (Vector), its polyclonal antibody (Vector) was incubated for 48 hours at 4°C at a dilution of 1:250 or 1:500. The injected superior cervical ganglion was used as a positive control.

Nitric oxide synthase (NOS) was demonstrated using a polyclonal antibody to brain NOS (Accurate Chemical and Scientific, Westbury, NY), incubated overnight at room temperature at a dilution of 1:5000. Brainstem and cerebral cortex were used as positive controls.

RESULTS

Pulleys and Smooth Muscle Distribution in Orbits of Monkeys and Humans

Orbital specimens of fascicularis and rhesus monkeys were serially sectioned for comparison with serial sections of two human orbits from different subjects. It was first necessary to determine whether the monkeys had rectus muscle pulleys comparable to those in humans. Coronal sections stained with Masson's trichrome (Fig. 1) demonstrate comparable EOM pulleys in humans and in both monkey species. Figure 1A shows a micrograph of a coronal section of a whole human orbit at the level of the densest part of the MR pulley; a complete ring of dense collagen encircles the MR tendon. Similar dense connective tissue rings are evident around the MR in the rhesus (Fig. 1B) and in the fascicularis (Fig. 1C) monkeys. Similar pulley rings were found for each of the rectus EOMs in all of the human and monkey orbits examined. As in human specimens, equatorial Tenon's fascia in both monkey species contained dense collagen (Fig. 1). The lateral levator aponeurosis, a connective tissue condensation that extends between the superior border of the lateral rectus pulley and the lateral border of the levator palpebrae superioris–superior rectus pulley complex, contained particularly dense collagen. Van Gieson's stain demonstrated elastin in equatorial Tenon's fascia, in the pulley sleeves, and in a dense deposit on the orbital side of each pulley in all human specimens. In the fascicularis monkey, elastin was particularly dense and diffusely distributed throughout pulley sleeves and especially in equatorial Tenon's fascia, in which the greatest thickness was approximately five times that of the sclera. Elastin was less abundant in the corresponding tissues of the rhesus monkey, although the relative thickness of equatorial Tenon's fascia was similar. The rhesus also exhibited cartilage in the connection between the MR and inferior rectus pulleys, as well as a cartilaginous promi-

nence extending from the trochlea along the reflected tendon of the superior oblique muscle. Neither monkey species exhibited a pulley around the accessory lateral rectus muscle, which inserted central to equatorial Tenon's fascia.

In paraffin-embedded and frozen sections of human specimens, immunoreactivity to human SM α-actin was highly specific to SM, with staining in striated EOMs limited to the walls of intrinsic blood vessels. In human specimens, immunoreactivity to SM α-actin was abundant in equatorial Tenon's fascia and in dense, focal bands running from pulleys to the adjacent orbital wall, to adjacent pulleys, and to the trochlea (Fig. 2A). A particularly dense band of SM was present in the lateral half of the lateral levator aponeurosis. The nasal portion of the lateral levator aponeurosis begins as a lateral extension of striated muscle fibers from the levator, which becomes contiguous approximately halfway along its course, with SM cells continuing laterally and inferiorly to the LR pulley. Another dense band of circumferential SM in human orbits extends from the inferior border of the MR pulley inferiorly to the medial border of the inferior rectus pulley. The majority of cells immunoreactive to SM α-actin had the characteristic spindle shape and Masson's trichrome staining of SM cells, although a few cells that were observed in collagen had branched morphology suggestive of myofibroblasts.

Smooth muscle α-actin immunoreactivity was specific in the fascicularis monkey, but SM cells were sparse in Tenon's fascia, except for a radial band near the equator of the globe. The most abundant SM in the equatorial Tenon's fascia of the fascicularis monkey was radially distributed, found around the MR pulley and extending to the inferior rectus pulley. In the rhesus, the SM α-actin antibody was cross-reactivative with striated EOMs (Fig. 2B), but cellular morphology permitted unambiguous identification. Radially oriented bands of SM were concentrated at the orbital side of the rhesus MR pulley, as they were in the human.

Synaptophysin and Myelin

Human orbital specimens in the vicinity of the MR pulley had immunoreactivity synaptophysin. These presumed synaptic end plates were identified in clusters on pulley SM. Myelin basic protein immunoreactivity was readily demonstrated in the larger orbital nerves in both human specimens but was never observed near or within the unmyelinated SM bands of rectus EOMs. This implies that, although the myelin antibody was reactive for larger nerves, the axon arborizations within pulley SM bundles are unmyelinated.

Sympathetic Innervation

To demonstrate sympathetic innervation, orbital tissues were immunostained for tyrosine hydroxylase, the rate-limiting enzyme in catecholamine biosynthesis. A rich distribution of axons immunoreactive to tyrosine hydroxylase was observed within SM bands in human (Fig. 3A) and rhesus (Fig. 3B) orbits. Immunoreactivity to dopamine β-hydroxylase indicates that the catecholamine pathway continues with conversion of dopamine to norepinephrine. Innervation in the rhesus superior rectus pulley SM contained dopamine β-hydroxylase (Fig. 4). In orbital and control human tissue, dopamine β-hydroxylase staining was unsuccessful, perhaps because of the delay between death and fixation of human tissue compared with the interval between death and fixation in the monkey tissue, which was perfused with fixative immediately after death. Monkey pulley SM tissue was not immunoreactive for phenylethanolamine-N-methyltransferase (not shown), indicating that catecholamine synthesis stops at norepinephrine, before epinephrine is synthesized, and that the sympathetic neurotransmitter that drives pulley SM is norepinephrine. The monkey adrenal medulla, in which epinephrine is synthesized, was a positive control observed to have immunoreactivity to all catecholamine synthetic enzymes.

Immunoreactivity to PHA-L was identified in the superior cervical ganglion and in nerves arborizing in SM around the rectus pulley in the rhesus that had earlier received PHA-L injection into the superior cervical ganglion. Figure 5 illustrates immunoreactivity for this tracer in small axons within rhesus superior rectus pulley SM. This finding indicates sympathetic projection from the superior cervical ganglion to the pulley SMs.

Parasympathetic Innervation

The AChE histochemical reaction demonstrated groups of typical, autonomic motor end plates within the macaque pulley SM (Fig. 6), suggesting parasympathetic, cholinergic innervation. As a control, acetylcholinesterase was also demonstrated in typical cholinergic motor end plates on monkey striated EOMs (not shown).

Nitroxidergic Innervation

Rich nitroxidergic innervation was demonstrated using the NADPH–diaphorase reaction in human (Fig. 7A) and rhesus (Fig. 7B) pulley SM. Axons were small, arborized, coiled within SM bundles, and ended in varicose motor end plates. A small amount of blue reaction product was often observed in SM around end plates, as illustrated in the double-stained preparation of Figure 7A, in which the SM bundle was confirmed by immunoreactivity to SM α-actin. Because the NADPH–diaphorase histochemical reaction is an indirect indication of the presence of NOS, direct confirmation was obtained by demonstration of immunoreactivity to NOS in axons innervating pulley SM of

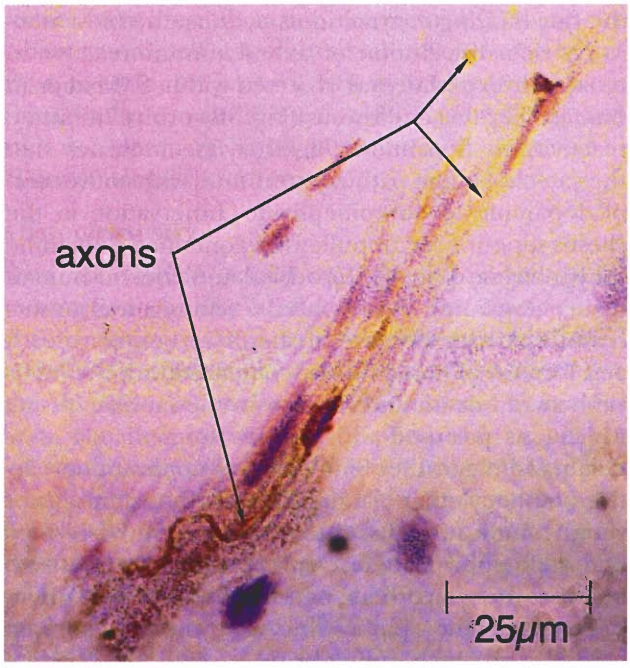

FIGURE 4. (*top left*) Varicose nerves are positive for dopamine β-hydroxylase immunoreactivity (brown peroxidase stain) in rhesus superior rectus pulley smooth muscle. Immunoreactivity was absent for phenylethanolamine-N-methyltransferase (not shown), indicating that the catecholamine synthesized is norepinephrine. Hematoxylin counterstain, oil immersion.

FIGURE 5. (*middle left*) After injection of PHA-L into superior cervical ganglion of rhesus monkey, immunoreactivity for this tracer was detected in small axons (*arrows*) within the SR pulley smooth muscles (*light brown*). This indicates a sympathetic projection from the superior cervical ganglion to pulley smooth muscle. Brown peroxidase stain.

FIGURE 6. (*bottom left*) Acetylcholinesterase histochemistry demonstrates multiple-beaded neuromuscular junctions along cholinergic nerves in bands of smooth muscle (*light purple*) near the rhesus superior muscle muscle. This suggests parasympathetic, cholinergic innervation of pulley smooth muscle. Hematoxylin counterstain, oil immersion.

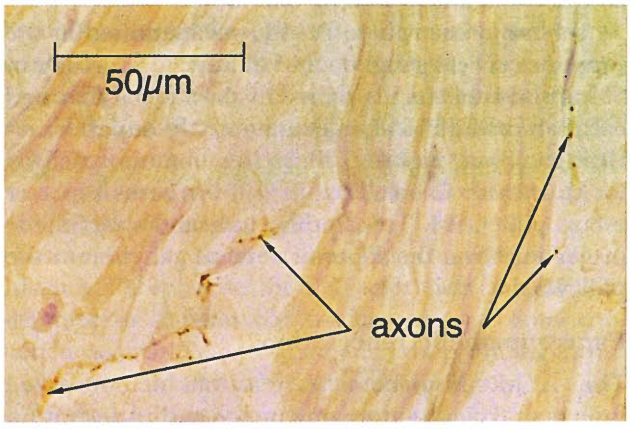

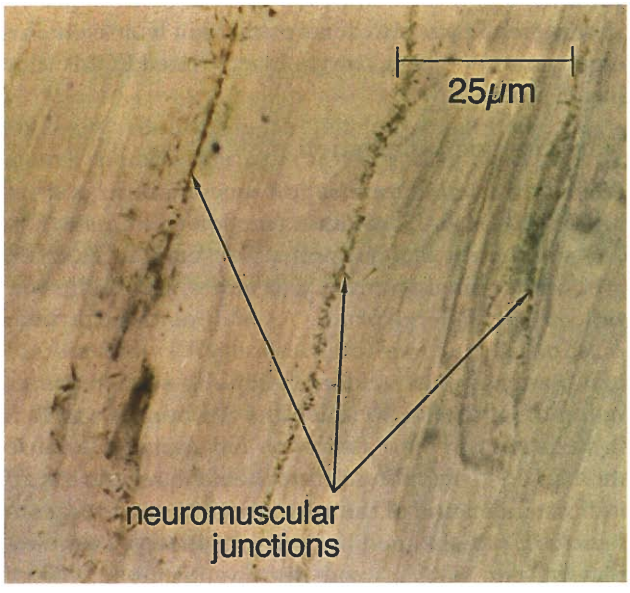

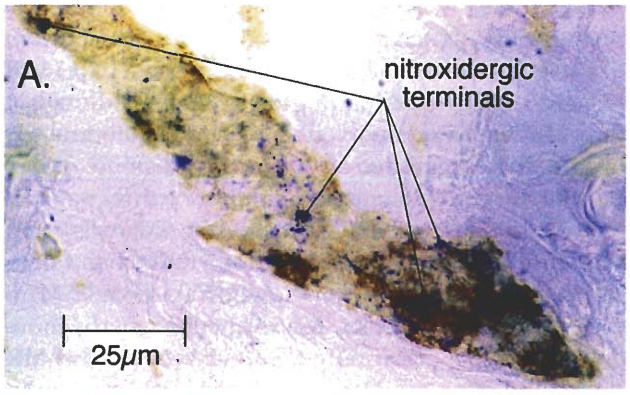

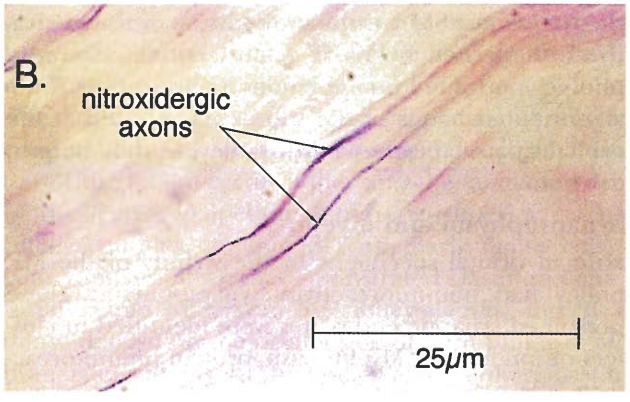

FIGURE 7. Frozen sections for NADPH–diaphorase histochemistry demonstrated nitroxidergic innervation (*blue*) in pulley smooth muscle. Oil immersion. (**A**) Smooth muscle bundle from human medial rectus pulley. NADPH–diaphorase-positive end plates (blue reaction product) terminate on smooth muscle demonstrated by immunoperoxidase stain for human smooth muscle α-actin (*brown*). (**B**) Multiple NADPH–diaphorase-positive axons in smooth muscle bundles near rhesus medial rectus pulley. Hematoxylin counterstain.

the macaque. Although axons in the SM were immunoreactive to NOS, staining was weaker than that for NADPH–diaphorase, reflecting a greater sensitivity of the enzyme histochemical technique.

The origins of the nitroxidergic innervation of pulley SM were sought. The midbrain and spinal cord of the rhesus were sectioned and stained for NADPH–diaphorase. Although a minority of midbrain neurons and fibers of passage were positive for NADPH–diaphorase, neurons in the Edinger–Westphal nucleus, the parasympathetic subdivision of the oculomotor complex, were negative. In humans (Fig. 8A) and rhesus monkeys (Fig. 8B), the pterygopalatine ganglion contained abundant somata and some fibers positive for NADPH–diaphorase. Immunoreactivity to NOS in the pterygopalatine ganglion mirrored NADPH–diaphorase activity (Figs. 8C, 8D).

The ciliary ganglion of the rhesus contained a few nitroxidergic somata, all located at the periphery of the ganglion. Adjacent serial sections in Figure 9 illustrate that the same neurons were positive for NADPH–diaphorase staining and NOS immunoreactivity. From the paucity of nitroxidergic somata in the ciliary ganglion, we do not think that the ciliary ganglion is a major source of nitroxidergic innervation to the orbit. Some other potential sources of nitroxidergic innervation were identified in serial sectioning of rhesus and human orbits. Small clusters of NADPH–diaphorase-positive ganglion cells were found within SM bundles of the rhesus MR pulley. These cells may comprise intrinsic nitroxidergic ganglia of the pulley SM.

Paraffin-embedded rhesus and human orbits were serially sectioned in the coronal plane from cornea to apex at 10-μm thickness. Ganglion cells were found in the inferior lateral orbital apex of both species, distributed either as a chain or as clusters of somata that appeared to be a rostral continuation of the pterygopalatine ganglion. These cells were NADPH–diaphorase positive, and may be the source of nitroxidergic innervation to pulley SM.

DISCUSSION

Pulleys of the extraocular muscles were present in both monkey species studied, differing in minor respects from those in humans. The human is more similar to the rhesus than to the fascicularis. In fascicularis, equatorial Tenon's fascia is thicker than in humans, and consists of collagen and dense elastin but little SM. Rhesus equatorial Tenon's fascia is also thick but contains less elastin and more SM than fascicularis. Cartilage also appears to contribute to the connective tissue structure in the rhesus. In humans, SM is widely distributed in equatorial Tenon's fascia and is prominent in condensations of SM arranged in bands extending from the elastin blocks of the MR pulley to the adjacent orbital wall and adjacent pulleys. The SM bands extend from the superior rectus to the lateral rectus pulleys and from the MR to the inferior rectus pulleys. In rhesus and humans, but not in fascicularis, radial bundles of SM join the MR pulley to the medial orbital wall. These distributions of SM were probably the ones grouped together by Müller under the term "peribulbar muscle." The comparative anatomic findings suggest that the physiologic function provided by stable pulley sleeves has adaptive value that is evolutionarily conserved, with varying arrangements of tissues in different primates. Perhaps distributed SM maintains stiffness of Tenon's fascia and the globe suspension into maturity, compensating for the progressive laxity of collagen and elastin. The abundance of SM in human orbits suggests that it is not a vestige inherited from nonhuman primates, but is an adaptation important to binocularity. Moreover, this argument is supported by the complete absence of the peribulbar SM in the rat,[14] a lateral-eyed animal.

We can speculate about a dynamic role for SM in the pulley suspensions. It is well positioned to modify EOM pulling directions, because pulleys function as mechanical origins of the muscles. A dynamic role in horizontal vergence is suggested by the most highly developed SM bands extending medially and anteriorly from the MR pulley to the anterior and posterior lacrimal crests in an arrangement that could produce anteroposterior movement of the pulley. A posterior movement of the MR pulley might facilitate convergence and adduction and prevent the MR pulley from interfering with vertical eye movements in the adducted position, in which the scleral insertion of the MR would otherwise approximate its pulley. Such posterior MR pulley movement, if actively produced, would be associated with relaxation of the prominent SM band during convergence. It is also possible that SM could play an important role in binocularity by finely tuning the static positions of the pulleys and the stiffness of Tenon's fascia. Computer simulations indicate that precise pulley positions are important to binocular yoking for near targets in three-dimensional space,[15] perhaps reducing the computational complexity of binocular kinematics faced by the brain.[22]

We have found a rich innervation of pulley smooth muscle in human and macaque orbits. The absence of myelin basic protein immunoreactivity and the fine caliber of axons terminating in pulley SMs indicate that the terminal innervation is not myelinated. These axons exhibit frequent bifurcations and varicosities, meandering extensively to

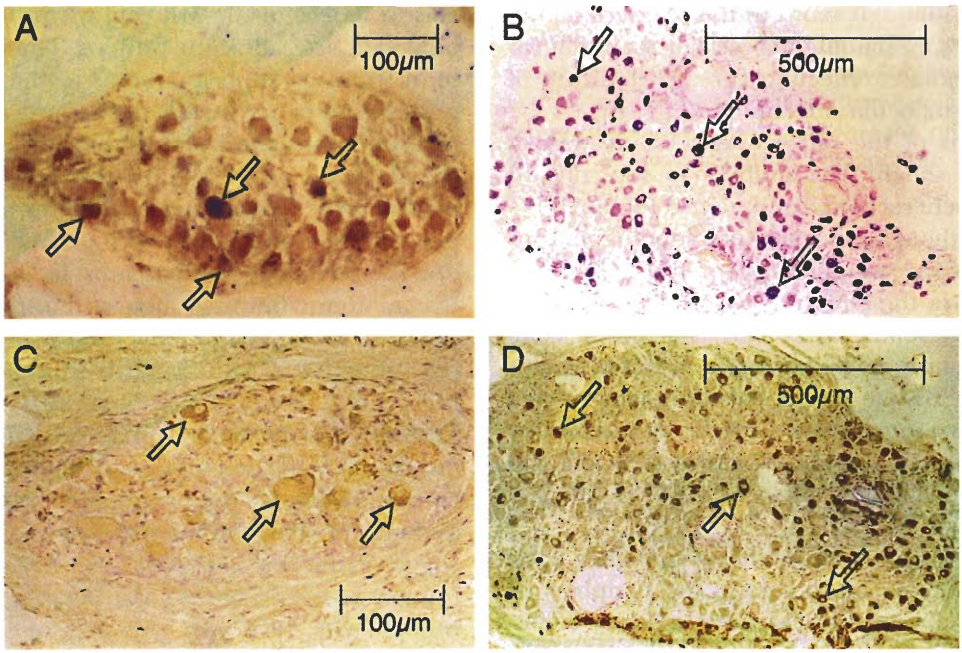

FIGURE 8.

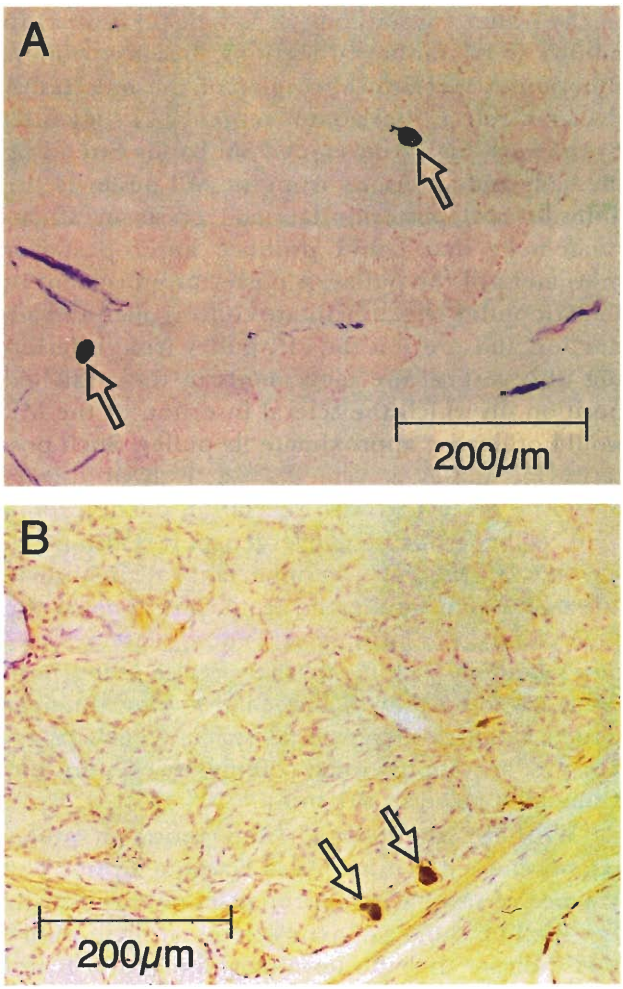

FIGURE 9.

terminate in clusters in pulley SMs. Such morphology is typical of autonomic innervation to SM.[23]

Sympathetic Innervation

We traced a sympathetic projection, which probably employs norepinephrine, to pulley SM from the ipsilateral superior cervical ganglion. This is consistent with the sympathetic projection to the superior tarsal (Müller's) muscle from the rostral ipsilateral superior cervical ganglion in such mammals as rat[24] and fascicularis monkey.[25] Electrical stimulation of the superior cervical ganglion in the alert rhesus may increase tension in the MR muscle (unpublished data), as we would expect from sympathetically induced contraction of the SM suspension of the MR pulley.

Parasympathetic Innervation

The ciliary and pterygopalatine are the two classically parasympathetic ganglia of the orbit. Baljet et al employed the AchE technique in the rhesus and fetal human to demonstrate parasympathetic projections from the pterygopalatine ganglion penetrating the orbital muscle and entering the orbit.[26] In agreement with the current findings, these investigators describe neuronal perikarya distributed along the major nerve trunks exiting the pterygopalatine ganglion. Parasympathetic projections from the ciliary ganglion mingle with those from the pterygopalatine ganglion to form an integrated retroocular plexus, which also contains scattered ciliary perikarya.[26] Thus, the current finding of AChE-positive innervation in pulley SM is consistent with a cholinergic, parasympathetic innervation of this muscle. The pterygopalatine and ciliary ganglia and scattered perikarya in the retroocular plexus are likely

FIGURE 8. Micrograph of 10-μm frozen sections demonstrating presence of nitroxidergic neurons in the pterygopalatine ganglion. (**A**) Several somata and fibers in portion of human pterygopalatine ganglion stain positively for NADPH–diaphorase (*purple, arrows*). (**B**) Numerous somata and some fibers in rhesus pterygopalatine ganglion stain positively for NADPH–diaphorase (*blue*). This elderly monkey had multiple calcifications (*large round structures*) in the pterygopalatine ganglion, as well as elsewhere in the orbit. (**C**) Nitric oxide synthase immunoreactivity (*brown, arrows*) in portion of human pterygopalatine ganglion is similar to NADPH–diaphorase (**A**). (**D**) Nitric oxide synthase immunoreactivity in rhesus pterygopalatine ganglion mirrors NADPH–diaphorase activity, as may be seen by comparison with (**B**). Hematoxylin counterstain.

FIGURE 9. Adjacent 10-μm sections demonstrating nitroxidergic neurons in rhesus ciliary ganglion. Hematoxylin counterstain. (**A**) NADPH–diaphorase stain demonstrates a few small positive neurons (*arrows*). Negatively staining ganglion cells (*light purple*) are considerably larger. (**B**) Nitric oxide synthase immunostaining labels similar small ganglion cells (*brown, arrows*).

sources of this parasympathetic innervation. However, in the rat, lesion of the ipsilateral superior cervical ganglion decreased the density of AChE-positive nerves in Müller's muscle, indicating that the superior cervical ganglion contributes to cholinesterase-positive innervation as well.[27] A possible cholinergic, sympathetic, postganglionic projection from the superior cervical ganglion to the pulley SMs can therefore not be excluded.

Nitroxidergic Innervation

Many SM systems, including vascular, intestinal, biliary,[28] and bladder,[29] are innervated by nonadrenergic, noncholinergic neurons that use the gaseous neuromessenger NO, which induces SM relaxation and mediates actions of other neurotransmitters. Nitric oxide is formed by the conversion by NO synthase of L-arginine to citrulline and NO, an enzyme now known to be identical to neuronal NADPH–diaphorase.[30] Toda et al provided direct evidence that NO acts as a neurotransmitter in the orbital vasculature, demonstrating after unilateral alcohol lesion near the pterygopalatine ganglion a loss of NADPH–diaphorase activity in the ganglion as well as abnormal responses of central retinal arterial strips to electrical and pharmacologic stimulation.[31] Nitric oxide controls arteriolar tone in the retina itself[32] and is abundant in neurons innervating the human ciliary SM and aqueous outflow pathway.[33] In rat, 10% to 15% of neurons in the ophthalmic division of the trigeminal ganglion and 70% to 80% of neurons in the pterygopalatine ganglion label positively for NOS.[34] Nitric oxide is involved in multiple local feedback loops involving mechanical forces. In response to local mechanical forces, vascular endothelium releases NO to relax vascular SM and regulate local blood pressure.[35] Nitric oxide synthase in the macula densa of the kidney functions as part of a local negative-feedback loop to control responses of the SM sphincter of the afferent arteriole and thus regulate local glomerular capillary pressure and glomerular filtration rate.[36] It is thus plausible that local mechanical feedback loops in Tenon's fascia, employing local release of NO, might serve to regulate connective tissue tension.

The presence of NO can be demonstrated with excellent sensitivity in nitroxidergic neurons using the NADPH–diaphorase reaction, and more specifically, using immunohistochemistry for the synthetic enzyme neuronal NOS.[30] The current study used these complimentary techniques to demonstrate that monkey and human pulley SMs have abundant nitroxidergic innervation, and revealed scattered nitroxidergic perikarya among the SM cells. Nitroxidergic axons in pulley SM appeared similar to those in vascular SM. In addition to the perikarya of the retroocular plexus, the pterygopalatine ganglion seems a likely source of nitroxidergic innervation of pulley SMs, because we found numerous nitroxidergic cells within that ganglion. These results are similar to findings in the rat.[34,37] Curiously, the pterygopalatine ganglion has historically been regarded as having a primary function in control of lacrimation and in rat receives preganglionic innervation from lacrimal and salivatory centers in the brainstem.[38] Nitroxidergic neurons in the pterygopalatine ganglion have also been shown to innervate the vessels of the circle of Willis in the rat.[34] Nitric oxide controls arteriolar tone in the retina itself,[32] and is abundant in neurons innervating the human ciliary SM and aqueous outflow pathway.[33] The ciliary ganglion was observed here in humans and monkeys to contain a few nitroxidergic perikarya, and so could also contribute to this innervation of pulley SMs. The absence in the current study of nitroxidergic neurons in the Edinger–Westphal nucleus rules out a direct nitroxidergic brainstem projection to pulley SMs.

In summary, the rectus EOMs of monkeys and humans pass through connective tissue sleeves that act as pulleys to influence EOM paths and act as functional origins of the striated muscles. Although the structure of the pulley tissues varies somewhat according to primate species, humans and rhesus monkeys have a peribulbar distribution of SM cells in equatorial Tenon's fascia, particularly near rectus pulleys. Embedded in equatorial Tenon's fascia, these SM cells suspending the rectus muscle pulleys receive rich, nonmyelinated sympathetic and parasympathetic innervation, probably employing norepinephrine, acetylcholine, and nitric oxide. Innervation of pulley SM appears typical of that of earlier-described orbital SMs. The sympathetic projection arises from the ipsilateral superior cervical ganglion, whereas the parasympathetic projections might arise from the pterygopalatine and ciliary ganglia and from scattered perikarya in the retroocular plexus. The pterygopalatine ganglion is probably the source of nitroxidergic innervation to pulley SM, although this remains to be demonstrated definitively. Antagonistic innervation of pulley SM suggests active neural regulation of pulley suspension stiffness, providing control of the paths and thus of the mechanical actions of striated extraocular muscles, thereby refining binocular coordination or aiding vergence eye movements.

Key Words

nitric oxide, orbit, parasympathetic innervation, pterygopalatine ganglion, sympathetic innervation

Acknowledgments

The authors thank William O'Day and Nicolasa De Salles for assistance with photomicrography.

References

1. Miller JM, Robins D. Extraocular muscle sideslip and orbital geometry in monkeys. *Vision Res.* 1987;27:381–392.
2. Simonsz HJ, Harting F, de Waal BJ, Verbeeten BWJM. Sideways displacement and curved path of recti eye muscles. *Arch Ophthalmol.* 1985;103:124–128.
3. Robinson DA. A quantitative analysis of extraocular muscle cooperation and squint. *Invest Ophthalmol.* 1975;14:801–825.
4. Miller JM. Functional anatomy of normal human rectus muscles. *Vision Res.* 1989;29:223–240.
5. Miller JM, Robinson DA, Scott AB, Robins D. Side-slip and the action of extraocular muscles. ARVO Abstracts. *Invest Ophthalmol Vis Sci.* 1984;25:182.
6. Miller JM, Demer JL, Rosenbaum AL. Two mechanisms of up-shoots and down-shoots in Duane's syndrome revealed by a new magnetic resonance imaging (MRI) technique. In: Campos EC, ed. *Strabismus and Ocular Motility Disorders.* London: Macmillian Press; 1990:229–234.
7. Miller JM, Demer JL. Biomechanical analysis of strabismus. *Binocular Vision Eye Muscle Surg Q.* 1992;7:233–248.
8. Miller JM, Demer JL, Rosenbaum AL. Effect of transposition surgery on rectus muscle paths by magnetic resonance imaging. *Ophthalmology.* 1993;100:475–487.
9. Simonsz HJ, Spekreijse H. Robinson's computerized strabismus model comes of age. *Strabismus.* 1996;4:25–41.
10. Demer JL, Miller JM, Poukens V, Vinters HV, Glasgow BJ. Evidence for fibromuscular pulleys of the recti extraocular muscles. *Invest Ophthalmol Vis Sci.* 1995;36:1125–1136.
11. Demer JL, Miller JM, Poukens V. Surgical implications of the rectus extraocular muscle pulleys. *J Pediatr Ophthalmol Strabismus.* 1996;33:208–218.
12. Porter JD, Poukens V, Baker RS, Demer JL. Structure-function correlations in the human medial rectus extraocular muscle pulleys. *Invest Ophthalmol Vis Sci.* 1996;37:468–472.
13. Müller H. Uber einen glatten Muskel in der Augenhohle des Menschen and dur Saugethiere. *Zwiss Zool.* 1858;9:541.
14. Page RE. The distribution and innervation of the extraocular smooth muscle in the orbit of the rat. *Acta Anat.* 1973;85:10–18.
15. Demer JL, Park CH, Howard TD, Miller JM. The oculomotor plant simplifies binocular yoking during vertical gaze shifts. ARVO Abstracts. *Invest Ophthalmol Vis Sci.* 1996;37:S165.
16. Kuntz A. The autonomic nervous system. In: Hartman CG, ed. *The Anatomy of the Rhesus Monkey.* Baltimore: Williams & Wilkins; 1933:328–338.
17. Sheehan DC, Hrapchak BB. *Theory and Practice of Histotechnology.* St. Louis: Mosby; 1973:95–116.
18. Vincent SR, Kimura H. Histochemical mapping of nitric oxide synthase in the rat brain. *Neuroscience* 1992;46:755–584.
19. Thompson SW. Microscopic histochemical methods for the demonstration of enzymes. In: *Selected Histochemical and Histopathological Methods.* Springfield, IL: Thomas; 1966:20.
20. Sternberger LA. *Immunocytochemistry.* New York: John Wiley & Sons; 1979:
21. Gerfen CR, Sawchenko PE. An anterograde neuroanatomical tracing method that shows the detailed morphology of neurons, their axons and terminals: Immunohistochemical localization of an axonally transported plant lectin, *Phaseolus vulgaris* leucoagglutinin (PHA-L). *Brain Res.* 1984;290:219–238.
22. Miller JM, Demer JL. New orbital constraints on eye rotation. In: Fetter M, Misslisch H, Tweed D, eds. *Three-Dimensional Kinematic Principles of Eye-, Head-, and Limb Movements in Health and Disease.* Tubingen: University of Tubingen; 1995:40.
23. Ehringer B. Adrenergic nerves to the eye and to related structures in man and in the cynomologous monkey (*Macaca irus*). *Invest Ophthalmol.* 1966;5:42–52.
24. Flett DL, Bell C. Topography of functional subpopulations of neurons in the superior cervical ganglion of the rat. *J Anat.* 1991;177:55–66.

25. van der Werf F, Baljet B, Prins M, Timmerman A, Otto JA. Innervation of the superior tarsal (Müller's) muscle in the cynomologous monkey: A retrograde tracing study. *Invest Ophthalmol Vis Sci.* 1993;34:2333–2340.
26. Baljet B, van dWF, Otto AJ. Autonomic pathways in the orbit of the human fetus and the rhesus monkey. *Doc Ophthalmol.* 1989;72:247–264.
27. Yamashita T, Honjin R. Fine structure, origin, and distribution of the autonomic nerve endings in the tarsal muscle in the eyelid of the mouse. *Cell Tissue Res.* 1982;222:459–465.
28. Kaufman HS, Shermak MA, May CA, Pitt HA, Lillemoe KD. Nitric oxide inhibits resting sphincter of Oddi activity. *Am J Surg.* 1993;165:74–80.
29. Thornburry KD, Hollywood MA, McHale NG. Mediation by nitric oxide of neurogenic relaxation of the urinary bladder neck muscle of the sheep. *J Physiol.* 1992;451:133–144.
30. Young HM, Furness JB, Shuttleworth CWR, Bredt DS, Snyder SH. Co-localization of nitric oxide synthase immunoreactivity and NADPH diaphorase staining in neurons of the guinea-pig intestine. *Histochemistry.* 1992;97:375–378.
31. Toda N, Ayajiki K, Yoshida K, Kimura H, Okamura T. Impairment by damage of the pterygopalatine ganglion of nitroxidergic vasodilator nerve function in canine cerebral and retinal arteries. *Circ Res.* 1993;72:206–213.
32. Donati G, Pournaras CJ, Munoz J, et al. Nitric oxide controls arteriolar tone in the retina of the miniature pig. *Invest Ophthalmol Vis Sci.* 1995;36:2228–2237.
33. Nathanson JA, McKee M. Identification of an extensive system of nitric oxide-producing cells in the ciliary muscle and outflow pathway of the human eye. *Invest Ophthalmol Vis Sci.* 1995;36:1765–1773.
34. Nozaki K, Moskowitz MA, Maynard KI, et al. Possible origins and distribution of immunoreactive nitric oxide synthase-containing nerve fibers in cerebral arteries. *J Cereb Blood Flow Metab.* 1993;13:70–79.
35. Himmel HM, Whorton AR, Strauss HC. Intracellular calcium, currents, and stimulus–response coupling in endothelial cells. *Hypertension.* 1993;21:112–127.
36. Wilcox CS, Welch WJ, Murad F, et al. Nitric oxide synthase in macula densa regulates glomerular capillary pressure. *Proc Natl Acad Sci USA.* 1992;89:11993–11997.
37. Yamamoto R, Bredt DS, Synder SH, Stone RA. The localization of nitric oxide synthase in the rat eye and related cranial ganglia. *Neuroscience.* 1993;54:189–200.
38. Ten Tusscher MPM, Klooster J, Baljet B, Van der Werf F, Vrensen GFJM. Pre- and post-ganglionic nerve fibers of the pterygopalatine ganglion and their allocation to the eyeball of rats. *Brain Res.* 1990;517:315–323.